Measurement of the quadrupole moments of the first $3/2^-$ and $5/2^-$ states of ^{109}Ag by Coulomb excitation

1973 J. Phys. A: Math. Nucl. Gen. 6 1571

(http://iopscience.iop.org/0301-0015/6/10/016)

J. Phys. A: Math., Nucl. Gen., Vol. 6, October 1973. Printed in Great Britain.

Measurement of the quadrupole moments of the first $3/2^-$ and $5/2^-$ states of ^{109}Ag by Coulomb excitation

D J Thomas, I Hall, M J Throop† and B Wakefield
Oliver Lodge Laboratory, University of Liverpool, PO Box 147, Liverpool, L69 3BX, UK

Received 22 March 1973

Abstract. The quadrupole moments of the 311 keV ($3/2^-$) and 415 keV ($5/2^-$) states of ^{109}Ag have been measured by the method of comparison of Coulomb excitation probabilities with two bombarding ions. The quadrupole moments of both states are negative, and at least that of the 311 keV state is large.

1. Introduction

The coupling of one or more particles to a vibrational core has been widely used in attempts to describe nuclei in mass regions in which nuclei are believed to be spherical. Calculations based on this model vary considerably in the degree of sophistication: from the weak coupling limit and one extra-core particle to intermediate coupling strengths and perhaps three extra-core particles. Our interest here is in the application of this model in the $A \simeq 100$ region.

In studies of odd-A nuclei some measure of success has been claimed for the model in reproducing the known properties of their excited states—principally level energies, spins and electromagnetic transition rates. Excited state quadrupole moments have not until now been considered in the comparison of model with experiment because they are not generally known.

In the case of even nuclei in this region, however, the measurements of the quadrupole moments of the first excited 2^+ states have aroused considerable interest. It is now well known that some of these moments are large whereas they should be zero according to the harmonic vibrational model. Although a detailed explanation of the measured moments is still awaited, the most promising approach so far seems to be that of Alaga *et al* (1967) and successive co-workers (Lopac 1970, Sips 1971). In this approach the anharmonicity which gives rise to the nonzero moments is ascribed to the interaction between extra-core particles and a harmonic vibrational core.

It appeared then that the model which was being invoked to explain the measured quadrupole moments of excited states of even nuclei was also the model which had been used for some time in attempts to explain level properties other than quadrupole moments in neighbouring odd nuclei. It seemed therefore highly desirable to fill in this gap in our knowledge of the odd-A nuclei.

We chose ^{109}Ag for study primarily for two reasons. Firstly the ground state is spin-$\frac{1}{2}$ and therefore has no spectroscopic quadrupole moment; this makes possible the measurement of excited state quadrupole moments by the same Coulomb excitation

† Now at: Physics Department, University of Oregon, Eugene, Oregon 97403, USA.

method by which those in neighbouring even nuclei have been measured. Secondly many of the electromagnetic transition strengths of the lower states in ^{109}Ag have been measured and these are needed in the analysis of the experiment. We report here measurements of the quadrupole moments of the first $3/2^-$ and $5/2^-$ states. These are the states which, in the simplest form of the model, arise from the coupling of a spin-$\frac{1}{2}$ particle (or hole) to a spin-2 phonon. In parallel with the experimental work described here we have been attempting to reproduce the properties of these and other low-lying negative parity states of ^{109}Ag in calculations using the particle–vibrator coupling model. These calculations and the implications of the present experimental results are discussed by Naqib *et al* (1973) in the following article.

2. Experiment

The static quadrupole moment of an excited state has a second-order effect on the Coulomb excitation probability of that state, the effect being approximately proportional to the mass of the bombarding ion. Thus for each of the two states we essentially compared the excitation probability measured with ^{16}O bombarding ions to that with ^{4}He ions. The apparatus and method was similar to, and developed from, that described by Christy *et al* (1970).

Ion beams of 33 MeV ^{16}O and 9 MeV ^{4}He from the Liverpool EN Van de Graaff generator were used to excite the 311 keV ($3/2^-$) and 415 keV ($5/2^-$) states. The targets were approximately 300 μg cm^{-2} thick and were prepared by evaporation of silver enriched to 99·7% ^{109}Ag onto copper and carbon backings. The latter were used respectively for ^{16}O and ^{4}He bombardment and were thick enough to stop the recoiling excited nuclei. This ensured that the decay γ rays were emitted from the well defined beam spot position on the target and also prevented the attenuation of the γ ray angular distribution which would occur if the excited nuclei were allowed to recoil in vacuo.

The $3/2^- \rightarrow$ ground and $5/2^- \rightarrow$ ground decay γ rays were counted in coincidence with ions scattered through a mean angle of 162° into an annular silicon surface barrier detector. A different γ ray detection system was used in each of three separate measurements of the ratio of ^{16}O:^{4}He induced coincidence yields. In two of these measurements 40 cm^3 Ge(Li) detectors were used and in both runs the detector was placed at an angle of 66° to the beam direction and 3·7 cm from the target. In the third run a 5·1 cm × 5·1 cm NaI(Tl) crystal was used at an angle of 58° to the beam direction and 3·0 cm from the target. In each case the γ ray detector was precisely positioned so that ^{16}O- and ^{4}He-induced yields were measured with the same counter geometry.

A conventional fast–slow coincidence electronics system was used. To improve the time resolution when using the Ge(Li) detectors we used the timing compensation technique described by Brandenberger (1969). Dead-time losses in time-to-amplitude converters and ADC's were reduced by fast coincidence gating. The most significant count-rate loss was then due to pile-up in the γ ray pulse height spectrum. This problem was the more serious in the first Ge(Li) run when the shaping of the γ ray pulses was set for optimal resolution (2·6 keV FWHM on the 415 keV line). In the second Ge(Li) run delay-line clipping was used to reduce pile-up and consequently the resolution was then somewhat worse (4·0 keV). However, optimum resolution was not needed in this experiment. Indeed, having established with the Ge(Li) measurements that there were no other significant peaks in the regions of the 311 keV and 415 keV lines in the spectrum (figure 1), we were able to make the third measurement using the NaI(Tl) detector

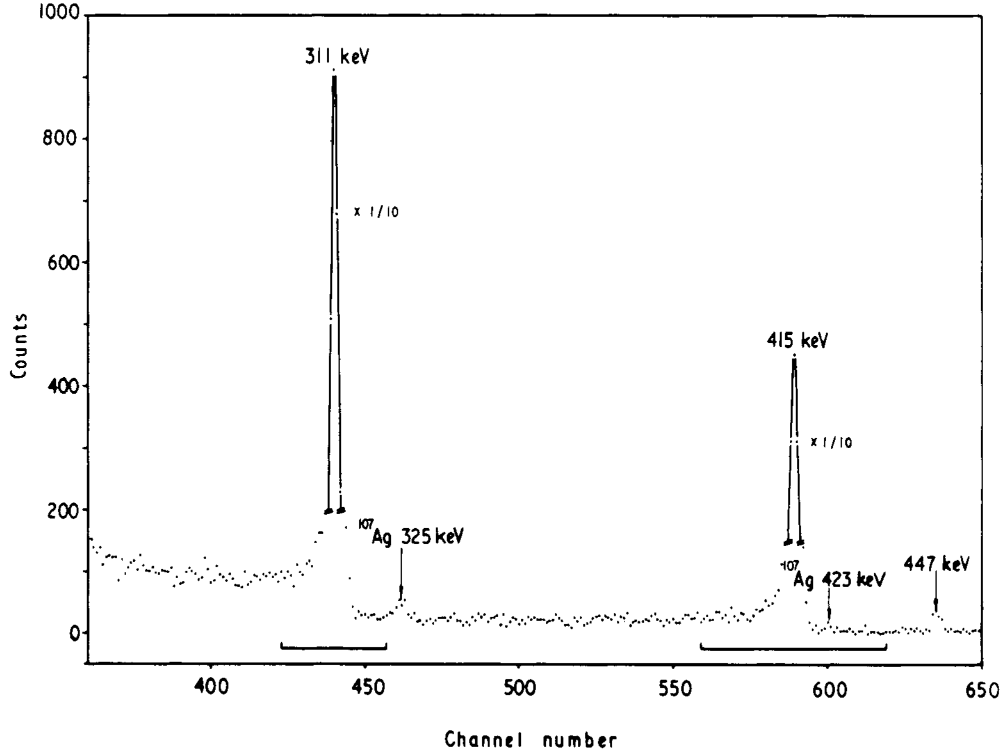

Figure 1. Spectrum of γ rays detected in a 40 cm^3 Ge(Li) crystal in coincidence with ^{16}O ions back-scattered from ^{109}Ag at a bombarding energy of 33 MeV. The horizontal bars indicate the widths over which the photopeak yields were evaluated.

which just resolved these two lines (figure 2). In the first Ge(Li) and NaI(Tl) measurements the count-rate losses were determined empirically by varying the beam current (figure 3). In the second Ge(Li) measurement, where the count-rate loss was small, the losses were measured by injecting into the counting system a known rate of pseudo particle–γ coincidence events using two synchronized pulse generators (Bolotin *et al* 1970).

Coincidence events were sorted in time and γ ray energy using an on-line computer. Spectra were electronically gated by a window set in the particle spectrum around the particle groups scattered elastically and inelastically from silver. The particle count in this window was taken with fast scalers. The photopeak count for each γ ray line was deduced after randoms subtraction by the further subtraction of a linear background interpolated from average backgrounds on either side of the peak. The ratio of the photopeak count to the particle count is called here the coincidence yield and is closely related to the excitation probability (see § 3). The final experimental datum from each run was the ratio of the coincidence yield measured with ^{16}O bombardment to that with ^4He. The ratios obtained in the three runs are given in table 1. Of course, the absolute coincidence yield deduced with either ^{16}O or ^4He is somewhat dependent on the method of background subtraction and on the number of channels in the γ ray spectrum over which the yield is evaluated. However, it is the ratio of the ^{16}O to ^4He induced yields which is the important quantity and this is insensitive to these factors.

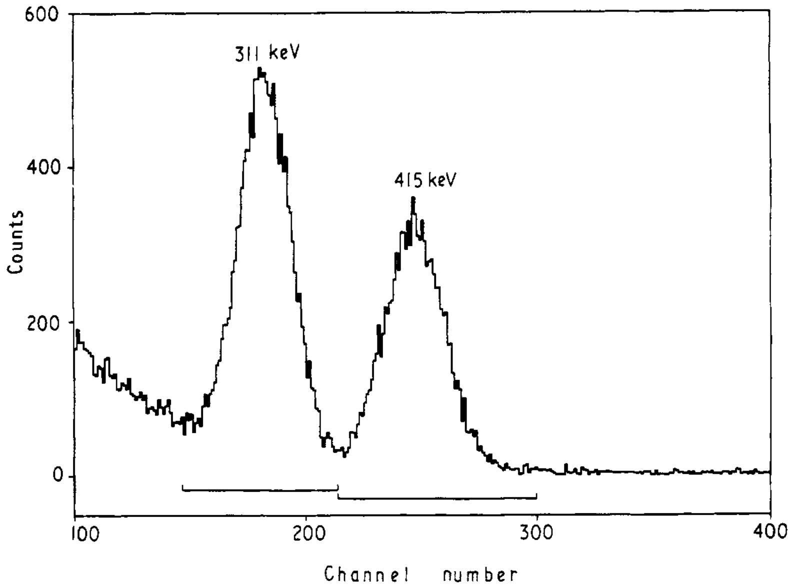

Figure 2. As for figure 1 but using a 5·1 cm × 5·1 cm NaI(Tl) crystal as the γ ray counter.

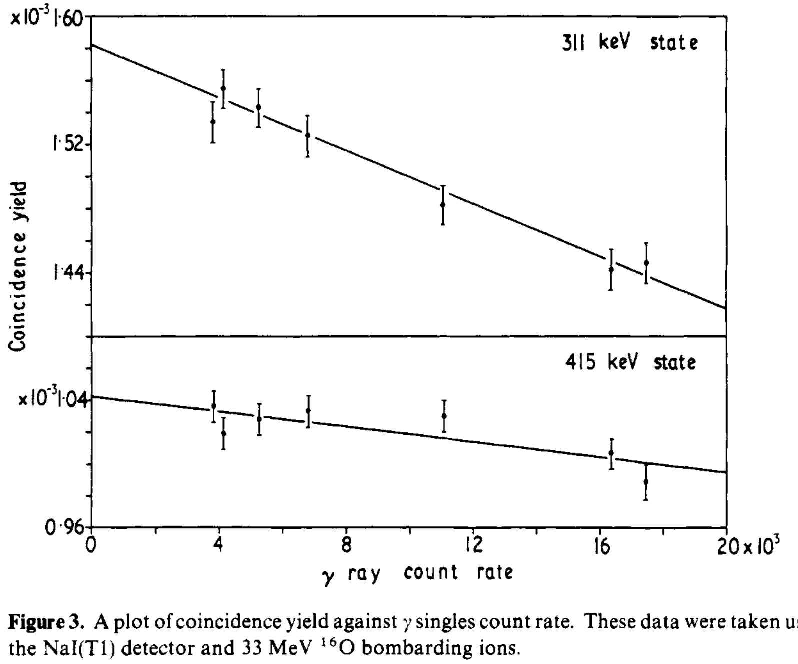

Figure 3. A plot of coincidence yield against γ singles count rate. These data were taken using the NaI(Tl) detector and 33 MeV ^{16}O bombarding ions.

The ratio given in table 1 for the 311 keV state in the NaI(Tl) run includes a correction allowing for the tail of the 415 keV line. The contribution of this tail in the window set round the 311 keV line was approximately 10 % but because the ratio of the 415 keV to 311 keV yields was very nearly the same for ^{16}O and ^{4}He bombardment the required correction was small ($\simeq$ 0·3 %).

Table 1. Ratios of the coincidence yield of the ground state decay γ ray induced by 32·60 MeV ^{16}O ions to that induced by 8·96 MeV ^{4}He ions. For counter geometries see text.

State	Ge(Li) 1	Ge(Li) 2	NaI(Tl)
311 keV ($3/2^-$)	$6{\cdot}63 \pm 0{\cdot}20$	$6{\cdot}62 \pm 0{\cdot}08$	$6{\cdot}60 \pm 0{\cdot}10$
415 keV ($5/2^-$)	$6{\cdot}32 \pm 0{\cdot}24$	$6{\cdot}54 \pm 0{\cdot}09$	$6{\cdot}38 \pm 0{\cdot}12$

The effective bombarding energy was taken to be the incident ion energy less half the target thickness. The latter was deduced for each target from measurement of the Rutherford scattering of ^{4}He ions.

3. Analysis

The coincidence yield of the 311 keV γ rays, for example, is predominantly due to the process of Coulomb excitation of the 311 keV state followed by γ ray de-excitation to the ground state. If one detected all the de-excitation γ rays and there were no other states in ^{109}Ag one would be measuring directly the excitation probability of the 311 keV state for the particular particle scattering angle used. In practice one may still deduce the excitation probability from the measured coincidence yield if one allows for the γ ray detector efficiency, the known γ ray angular distribution and the effects of other excited states.

In this experiment the γ ray angular distribution in the case of ^{16}O bombardment is very nearly the same as that in the case of ^{4}He bombardment. This is partly a feature of the Coulomb excitation process and partly due to the particle scattering angle being close to 180°.

The other excited states affect the measured coincidence yield in two ways. Firstly the excitation probability of the state is modified slightly by higher-order excitations which proceed virtually through the other states; secondly the yield of the decay γ rays is enhanced slightly by the excitation and cascade decay of higher states.

These effects are readily computed with the de Boer–Winther Coulomb excitation program which was used in the analysis. The levels of ^{109}Ag which were included are shown in figure 4. The E2 matrix elements used are given in table 2. They are based on the B(E2) values given by Robinson *et al* (1970) with the exceptions of those indicated with footnotes and those ($r, s \geqslant 4$) set equal to zero; none of the matrix elements in these two groups significantly affect the analysis.

As noted in the first paragraph it is possible first to deduce excitation probabilities from the data and then, in a second stage of the analysis, to deduce the quadrupole moments. However, it is more direct and convenient to compute theoretical values of the experimental ratios in the following way. The angular distribution of de-excitation γ rays is

$$\frac{\mathrm{d}W(\theta)}{\mathrm{d}\Omega} = A_0 + A_2 P_2 + A_4 P_4$$

where P_2 and P_4 are Legendre polynomials and the coefficients $A_0 A_2$ and A_4 are computed with the de Boer–Winther program. This expression then includes the small

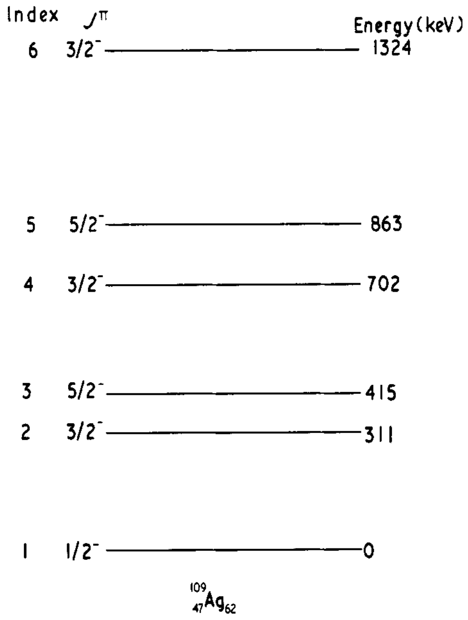

Figure 4. The energy levels of ^{109}Ag which were included in the analysis.

Table 2. The E2 matrix elements used in the analysis. The level indices are as shown in figure 4. The matrix elements are defined by

$$M_{rs} = \langle s \| i^{\lambda}\mathcal{M}(E\lambda) \| r \rangle = (-1)^{\lambda+I_r-I_s}\langle r \| i^{\lambda}\mathcal{M}(E\lambda) \| s \rangle$$

where $\mathcal{M}(E\lambda)$ is the multipole operator and $\lambda = 2$. $M_{rs}^2 = (2I_r+1)B(E2, r \rightarrow s)$ and the quadrupole moments of the 3/2⁻ and 5/2⁻ states are given by

$$Q(3/2^-) = -0{\cdot}709\, M_{22}$$

$$Q(5/2^-) = -0{\cdot}774\, M_{33}$$

Level index *s* / *r*	1	2	3	4	5	6
1	0	−0·67	−0·80	−0·04	−0·19	−0·16
2	0·67	M_{22}	∓0·22	−0·21[a]	∓0·33	−0·07
3	−0·80	±0·22	M_{33}	−0·33[a]	∓0·36	−0·27[b]
4	0·04	−0·21[a]	0·33[a]	0	0	0
5	−0·19	±0·33	∓0·36	0	0	0
6	0·16	−0·07	0·27[b]	0	0	0

a From estimates given by Robinson *et al* (1970) based on a phonon-mixing model of ^{109}Ag.
b Upper limit based on the experiments of Robinson *et al* (1970).

effects of other excited states. The coincidence yield measured with a γ ray detector at some angle θ is therefore

$$y(\theta) = G_0A_0 + G_2A_2P_2 + G_4A_4P_4$$

where $G_0/4\pi$ is the detector efficiency and $G_2/G_0 = J_2$ and $G_4/G_0 = J_4$ are the angular distribution attenuation coefficients of the detector. Using singly and doubly primed symbols to signify respectively ^{4}He and ^{16}O bombardment, the measured ratio is

$$R = \frac{y''(\theta)}{y'(\theta)} = \frac{A_0''+J_2A_2''P_2+J_4A_4''P_4}{A_0'+J_2A_2'P_2+J_4A_4'P_4}. \tag{1}$$

The attenuation coefficients J_2 and J_4 are dependent on γ ray energy. Thus the coefficients appropriate to the 415 keV γ ray are slightly different from those for the 311 keV γ ray, the values actually used being approximately $J_2 = 0{\cdot}90$, $J_4 = 0{\cdot}69$ for the two similar Ge(Li) detectors and $J_2 = 0{\cdot}85$, $J_4 = 0{\cdot}52$ for the NaI(Tl) detector. From our earlier remarks on the similarity of the γ ray angular distributions it may be seen from equation (1) that the ratio R is insensitive to the precise values of these coefficients. In the cascade contributions to the coincidence yield the difference between ^{16}O and ^{4}He bombardment was in no case more than 0·5 %, and in the effect of the γ ray angular distribution the difference was at most 0·3 %.

For each of the two states under study values of R were computed with trial values of the diagonal E2 matrix element M_{ii} for that state. A value of M_{ii} and hence the quadrupole moment was then found from the experimental value of R by interpolation, the dependence of R on M_{ii} being very nearly linear over a sensible range of M_{ii}.

Although the E2 transition rates in ^{109}Ag which are needed for the analysis have been measured, the relative phases of the matrix elements are not known. In the multiple Coulomb excitation of a state there are therefore interference terms (other than that due to the quadrupole moment) whose signs are unknown. The deduced quadrupole moment therefore depends on the signs assumed for the various matrix elements. Thus the analysis outlined above was carried out separately for different combinations of signs. In practice there were two matrix elements in each case whose signs had a significant effect, namely, M_{23} and M_{25} in the case of the 311 keV state and M_{23} and M_{35} in the case of the 415 keV state.

The data from the two Ge(Li) measurements were combined before analysis since these were made with the same counter geometry. The results are given in table 3. The quoted errors are predominantly due to counting statistics although in table 3(*b*) the small error due to target thickness uncertainty has been included. The stated errors do not, however, take account of the uncertainties in the matrix elements shown in table 2; we prefer to keep experimental error separate from uncertainty in analysis. The only significant uncertainty derives from the errors in the values of M_{23}, M_{25} and M_{35} which are respectively about 40 %, 15 % and 20 %. (These matrix elements correspond to transitions between excited states and these are difficult to measure accurately.) A 40 % change in M_{23}, for example, would result approximately in a similar change in the difference between the values of Q_2 deduced with opposite signs of M_{23}.

We have assumed that the excitation process is exclusively E2. Parity conservation rules out first order excitation by E1 or E3 processes and M1 excitation is negligibly weak. In principle excitation may proceed via positive parity states but the likeliest case would be excitation of the $5/2^-$ state by a second-order E3–E1 process through the 88 keV $7/2^+$ state; but even this is an extremely weak process.

4. Conclusion

It appears that both the first $3/2^-$ and $5/2^-$ states of ^{109}Ag have negative quadrupole moments. Furthermore, and despite the uncertainties in some of the E2 matrix elements used in the analysis, we may conclude that the $3/2^-$ state at least has a large quadrupole moment. For comparison we note that if this state was a member of a rotational band based on the ground state the magnitude of the quadrupole moment would be about 0·5 eb. The results are discussed in more detail in the following article.

Table 3. Quadrupole moments of 311 and 415 keV states of ^{109}Ag.

(*a*) Diagonal E2 matrix elements of the first $3/2^-$ and $5/2^-$ states of ^{109}Ag deduced from the Ge(Li) and NaI(Tl) measurements, and their dependence on the phases of other matrix elements

311 keV ($3/2^-$) state

M_{23}	M_{25}	M_{22} (eb)		
		Ge(Li)	NaI(Tl)	Weighted mean
−	−	0·88 ± 0·19	0·89 ± 0·28	0·88 ± 0·16
−	+	1·02 ± 0·19	1·04 ± 0·27	1·03 ± 0·16
+	−	1·25 ± 0·18	1·26 ± 0·26	1·25 ± 0·15
+	+	1·38 ± 0·18	1·39 ± 0·26	1·38 ± 0·15

415 keV ($5/2^-$) state

M_{23}	M_{35}	M_{33} (eb)		
		Ge(Li)	NaI(Tl)	Weighted mean
−	+	0·17 ± 0·21	0·54 ± 0·32	0·29 ± 0·18
+	+	0·33 ± 0·21	0·68 ± 0·31	0·44 ± 0·17
−	−	0·41 ± 0·21	0·78 ± 0·31	0·52 ± 0·17
+	−	0·56 ± 0·21	0·91 ± 0·31	0·67 ± 0·17

(*b*) Summary of results for the quadrupole moments Q (eb)

M_{23}	M_{25}	M_{35}	$Q\,(3/2^-)$	$Q\,(5/2^-)$
−	−	−	−0·63 ± 0·13	−0·40 ± 0·16
−	+	+	−0·74 ± 0·13	−0·22 ± 0·16
+	−	−	−0·89 ± 0·13	−0·52 ± 0·16
+	+	+	−0·98 ± 0·13	−0·34 ± 0·16

Acknowledgments

We thank A Christy, R P Harper, and M Nolan for their help in collecting the data. MJT thanks the University of Liverpool for a research fellowship. This work was supported by the Science Research Council.

References

Alaga G, Krmpotic F and Lopac V 1967 *Phys. Lett.* **24B** 537–9
Bolotin H H, Strauss M G and McClure D A 1970 *Nucl. Instrum.* **83** 1–12
Bradenberger J D 1969 *Nucl. Instrum.* **69** 271–6

Christy A *et al* 1970 *Nucl. Phys.* A **142** 591–603
Lopac V 1970 *Nucl. Phys.* A **155** 513–25
Naqib I M, Thomas D J and Wakefield B 1973 *J. Phys.* A: *Math., Nucl. Gen.* **6** 1580–93
Robinson R L *et al* 1970 *Nucl. Phys.* A **150** 225–46
Sips L 1971 *Phys. Lett.* **36B** 193–5